Titre: Title:	Influence of soil-structure interaction on seismic demands in shear wall building gravity load frames
Auteurs: Authors:	Mathieu Choinière, Patrick Paultre, & Pierre Léger
Date:	2019
Type:	Article de revue / Article
Référence: Citation:	Choinière, M., Paultre, P., & Léger, P. (2019). Influence of soil-structure interaction on seismic demands in shear wall building gravity load frames. Engineering Structures, 198. https://doi.org/10.1016/j.engstruct.2019.05.100

Titre de la revue: Journal Title:	Engineering Structures (vol. 198)
Maison d'édition: Publisher:	Elsevier
URL officiel: Official URL:	https://doi.org/10.1016/j.engstruct.2019.05.100

In uence of soil-structure interaction on seismic demands in shear wall building gravity load frames

Mathieu Choinière[a], Patrick Paultre[a], Pierre Léger[b]

[a]Department of Civil Engineering, University of Sherbrooke, 2500 Blvd de l'Université, Sherbrooke, QC, Canada J1K 2R1.
[b]Department of Civil, Geological and Mining Engineering, École Polytechnique, 2500 chemin de Polytechnique, Montréal, QC, Canada H3C 3A7.

Abstract

This paper presents a complete and simple linear method, with a suitable force modi cation factor, to compute seismic demands in the gravity load resisting system (GLRS) of shear wall buildings including foundation movement. Based on the method rst proposed by Beauchamp, Paultre and Léger in 2017, this paper compares two approaches to consider foundation movement on linear soil media such as (a) a simple rotational spring under each core and (b) a complete set of springs and dashpots. A xed-base model using code foundation factors is also used for comparison. Springs and dashpots are assessed by modelling soil-structure interaction (SSI) with solid nite elements. Then, these approaches are evaluated for a typical 12-storey concrete shear wall building considering several nonlinear time history analyses (NLTHAs). SSI is modelled with a set of springs and dashpots, and ground motions are selected from the conditional spectrum method. NLTHAs are performed for soil classes ranging from stiff to soft, and the effect of the underground structure cracking is analysed. Analysis results show that the proposed methods are accurate in computing seismic demands in the GLRS compared to NLTHA. Foundation movements should be explicitly modelled for soil class D or softer, and underground structure cracking should be considered. For the very soft soil class E, the behaviour of the building is poorly captured in linear analysis methods; thus, nonlinear analyses are required.

Keywords:
Reinforced concrete, building, gravity load resisting system, soil-structure interaction, seismic design, nonlinear time history analysis, conditional spectrum

1. Introduction

In North America, reinforced concrete (RC) buildings must have a seismic force resisting system (SFRS) that shall be able to resist 100% of seismic forces [1, 2]. The design of elements part of the SFRS is somewhat straightforward and generally well known to engineers. Even if the SFRS can carry all induced seismic loads, the other structural elements of the building, the gravity load resisting system (GLRS), are deformed by oor slab movements during

Corresponding author: Department of Civil Engineering, University of Sherbrooke, 2500 Blvd de l'Université, Sherbrooke, QC, Canada J1K 2R1. Tel.:+1 819 821-7108.
Email address: Patrick.Paultre@USherbrooke.ca (Patrick Paultre)

an earthquake. The seismic design of elements part of the GLRS must be performed during the building design process because its importance has been well recognized from past major events. During the Northridge earthquake in 1994 [3], the Haiti earthquake in 2010 [4] and the Christchurch earthquake in 2011 [5], some components that were supposed to carry only gravity loads failed, leading to the collapse of buildings they were part of. Indeed, the failure of one or more elements of the GLRS is known as one of the most common causes of building collapse during an earthquake.

Both the Canadian design of concrete structures standard CSA A23.3-14 [6] and the American Concrete Institute code ACI 318-14 [7] state that the GLRS must withstand the large deformations induced by earthquakes. This is to ensure that the elements part of the GLRS have either sufficient capacity to deform elastically or sufficient ductility to carry gravity loads in their deformed shapes. To achieve this, the building needs to be analysed in its deformed configuration, which includes the effects of torsion, cracked section properties and foundation movements. Recently, Adebar et al. [8] showed that using a linear model to calculate the drift profile of shear wall buildings, ignoring inelastic deformations, can lead to a significant underestimation of seismic forces in gravity columns, principally in the first storeys. In response to this problem, CSA A23.3-14 requires that the design displacement incorporate the inelastic displacement profile of the SFRS. Because of the complexity of this requirement, a simplified method based on the research of Ghezhdar [9] is proposed in CSA A23.3-14 [6]. Recently, a simple and more direct method based on a single linear model of the complete building was proposed by Beauchamp et al. [10].

Regarding the inelastic displacement profile, the interaction of a building with the soil underneath is often not explicitly considered by engineers. Seismic hazard maps in Canada and in the United-States have been developed for structures sitting directly on rock sites and firm ground. However, most buildings are constructed given soil conditions that can affect the response of structures founded on them. For example, during the Chi-Chi earthquake in 1999, some buildings well resisted the earthquake but ultimately collapsed because the soil lost its capacity [11]. Moreover, during the Saguenay earthquake in 1988, buildings further away from the epicenter were damaged more so than certain buildings closer to the epicenter because they were constructed on soft soil [12]. In North American standards, the dynamic effects of soil are considered using modification factors on the seismic excitation, but the movement of the soil deposit itself is rarely considered. The consideration of this effect for shear wall concrete buildings generally decreases the forces in the walls, but it increases displacements and thus the deformation of secondary elements of the GLRS [13]. Requirements of CSA A23.3-14 and ACI 318-14 also note to that effect Foundation movements must be considered in the displacement profile used for the computation of seismic demands in the GLRS [6, 7].

This paper compares two approaches to consider foundation movements to extend the method proposed by Beauchamp et al. [10]: (1) a single rotational spring under each wall and (2) a complete set of springs and dashpots. These approaches are also compared with a fixed-base model. Their accuracy and efficiency are evaluated for a typical shear-wall 12-storey building using the results of several nonlinear time history analyses (NLTHAs) in which ground motions are selected and scaled from the conditional spectrum method. NLTHAs are performed for soil classes ranging from stiff to soft, and the effect of underground structure cracking is investigated. Additionally, all analyses

are used to assess the simplified method suggested in CSA A23.3-14 extended to include foundation movements.

The scope of this paper is limited to assessing the influence of the flexibility of a linear homogeneous soil deposit on the seismic demands in GLRS. Uplift of the foundation is not considered, even though it has been verified that no uplift occurs in the studied models. Seismic demands in the GLRS are presented only for columns, although the proposed method is also efficient for other elements. The effects of torsion on the determination of seismic demands in the GLRS have been studied by Beauchamp et al. [10]; thus, torsion is not included in the present paper to simplify calculations and to focus on the effects of flexible soil conditions.

2. Seismic design of GLRS

2.1. Requirements of the ACI 318-14

The ACI 318-14 requirements for the seismic design of the GLRS focus more on the detailing of members than on a refined procedure to calculate seismic demands in the GLRS. Members not designated as part of the SFRS must be designed to sustain the factored gravity loads ($1.2D + 1.0L + 0.2S$ or $0.9D$) acting simultaneously with the lateral displacement expected for the design-basis earthquake [7]. Even if it is not required to consider the inelastic displacement profile, the intention of ACI 318-14 and the standard ASCE 7-16 [1] is to encourage engineers in providing intermediate or special detailing in beams and columns that are not part the SFRS. This approach is based on observations and experimental evidence that well-detailed structural elements can endure large inelastic deformations without losing significant vertical load-carrying capacity [11]. The ACI 318-14 requirement even permits one to not explicitly check the effect of the design displacement on gravity members if special detailing requirements are provided [7].

2.2. Simplified method in CSA A23.3-14

Unlike ACI 318-14, CSA A23.3-14 requires one to consider the inelastic displacement profile in computing the seismic demands in the GLRS. This requirement can be achieved by analysis using a simplified method for concrete buildings in which the SFRS consists of shear walls [6]. The curve labelled "cantilever wall" shown in Fig. 1 is proposed to evaluate the inelastic displacement profile based on the global drift ratio Δ_w/h_w, where h_w is the height of the building and Δ_w is the design displacement at the top of the GLRS.

Curves corresponding to the moment-resisting frame and coupled wall were added later in CSA A23.3-14 Explanatory Notes in the CAC Concrete Design Handbook [14]. However, this method is limited to buildings with simple SFRS. A building with two types of SFRS in the same loading direction can hardly be analysed following that procedure. Moreover, a single displacement profile is rarely sufficient because the design displacement at the top of the building varies because of torsion.

2.2.1. Consideration of foundation movements

In some cases, the foundation of a building is restrained against rotation by a structure that is shown to have sufficient stiffness and strength. Is this case, it is not required to consider foundation movements [6]. On the other

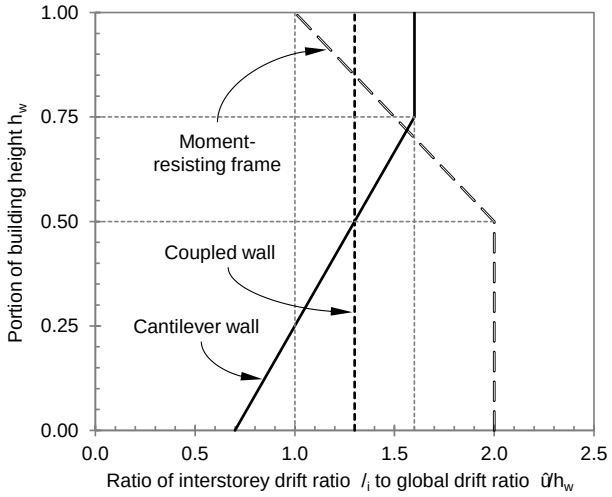

Figure 1: Envelop of relative interstorey drift ratios for the simpli ed analysis in CSA A23.3-14.

hand, the rotation of exible foundations must be considered in the calculation of the design displacement. For foundations designed in accordance with the capacity design principle, their rotation can be computed based on the overturning moment according to Eq. 1. This equation, proposed in CSA A23.3-14, is a simpli ed version of a procedure developed by Adebar [15].

$$= 0.3 \frac{q_s}{G_0} \left(\frac{`_f}{a_s} \right)^{1.5} \left(1 + 2 \frac{a_s}{b_f} \right) \quad (1)$$

where is the foundation rotation in radians, b_f and $`_f$ are the width and length of the footing, respectively, and q_s are the length and magnitude of the uniform bearing stress in soil required to resist the applied loads, G_0 is the maximum shear modulus of the soil for small strains. To consider foundation movements in the computation of the building displacement pro le, it is recommended that the rotation, in radians, be added at every level to the interstorey drift ratio determined from a xed-base model [16].

2.3. Method proposed by Beauchamp et al. [10]

Beauchamp et al. [10] proposed a more general method to determine seismic demands in the GLRS. The method requires a single linear model of the building that can be used to facilitate the seismic design of both the GLRS and the SFRS based on modal response spectrum analysis (RSA). The method consists of modelling the complete building and reducing the sti ness of the elements part of the GLRS; therefore, they do not attract the behaviour of the SFRS. This reduction factor (F_{sr}) can be taken between 10^{-2} and 10^{-3}. The model is then identi ed as gravity nearly null sti ness (GNS). The forces in elements part of the GLRS is directly computed for each mode and combined with the appropriate method. These forces are very small because of the reduction factor applied; therefore, the design forces in the GLRS are obtained by multiplying inversely:

$$F_{SRCG} = F_{GNS} \frac{1}{F_{sr}} \frac{V_d}{V_e} \frac{R_d R_o}{I_e} \quad (2)$$

where V_d/V_e is a ratio representing ductility and overstrength. Because the forces in the GLRS are caused by the displacement of the structure, they are increased by the ratio $R_d/R_o = I_e$, as recommended in NBCC 2015 [2]. [The latter can be viewed as the Canadian equivalent to the ratio C_d/I_e in ASCE 7-16 [1].

To consider the inelastic displacement profile of the SFRS, Beauchamp et al. [10] suggested, following comprehensive parametric analyses, to further reduce the stiffness of walls in the plastic hinge zone, giving the linear plastic hinge (LPH) model. They used an effective elastic modulus of $E_{eff} = 0.35E_c$, which is half the value assigned to the remainder of the walls. Dezhdar [9] in contrast suggests to use approximately half that value but applied to approximately half the length of the wall.

As presented, this method does not consider foundation movement. As will be discussed in Section 3, the flexibility of the foundation generally increases displacements in the structure, which increases forces in the GLRS. Thus, it is important to evaluate the influence of the foundation movements on the GLRS and improve the proposed simplified method accordingly [10].

3. Soil-structure interaction

Every building is supported by a soil foundation having stiffness, damping and mass properties. Therefore, it is important to understand how soil properties modify the behaviour of the structure above. A distinction should be made between site effects and soil-structure interaction (SSI). In rock foundations we observe high frequency free-field motions, because this stiff media is able to transmit them up to the surface. In soft soil, high frequency motions are filtered out, the amplified free-field response is then taking place in the longer period range. Therefore, the seismic input motions depends on the depth and stiffness of the soil deposit according to the site class. This is known as site effect and does not involved interaction with the building structures. Herein, we apply the 2015 National Building Code of Canada (NBCC) [2] site modifications factors (similar to the American Society of Civil (ASCE) [1]) to adjust the spectral ordinates of the target uniform hazard spectra (UHS) for soil classes C to E. On the other hand, SSI has three principal effects on the design of structures: (1) Inertia and flexibility of the soil deposit modify dynamics properties of the complete system; (2) kinematic effects of SSI modify free-field ground motions in a different signal at the base of the foundation, and (3) the deformation of the soil can increase displacements in the structure and modify forces in structural elements [16]. The first and the last effect can be regrouped in the inertial interaction, while the second one is the kinematic interaction.

In North American standards, the kinematic interaction is somewhat considered using modification factors in the seismic excitation that depend on the intensity of the loading and on the soil class [1, 2]. On the other hand, inertial interaction is rarely considered, as it is generally accepted that it is safe not to do so. Indeed, considering the flexibility of the soil deposit lengthens the fundamental period of the soil-structure system, most often leading to a reduction in the seismic excitation. However, even if it decreases forces in the walls for concrete buildings, considering the flexibility of the soil can increase displacements and thus the deformations of components of the GLRS [13]. Tahi

et al. 2014 [17] studied the adequacy of considering only site effects excluding SSI as compared to including SSI for moment resisting frame buildings ranging from 5 to 15 storeys. Soil site class D with average shear wave velocity in the top 30 m of soil, $\bar{V}_s$, equal to 320 m/s and class E with $\bar{V}_s$ = 150 m/s were investigated. It was concluded that it was acceptable to exclude SSI for site class D, to estimate structural displacements. Neglecting SSI to estimate building base shears for site D, and both displacements and base shears for relatively soft soil E was on the unsafe side. To model SSI and its effects, two main methods are described in the literature [13, 16]. The first method is called the direct method, and the other method is the substructure method. Both methods are briefly described in Subsections 3.1 and 3.2.

3.1. Direct method

The direct method consists of a complete modelling of the system soil-foundation structure, as shown in Fig. 2. A large soil deposit discretized in small finite elements must be modelled with appropriate properties. This method is the most accurate, as the dynamic behaviour of the entire system is directly obtained. However, it remains computationally expensive and time consuming; therefore, it is rarely used by practising engineers [13]. Several challenges arise in regard to performing a time history analysis of a structure in which SSI is modelled by the direct method:

(1) Properties of soil finite elements should be defined with care. An adequate modelling of wave propagation is important, and an equivalent linear representation of the soil properties is often used to this end [16].

(2) Boundary conditions of the soil deposit must be well defined so that they do not modify the behaviour of the structure. In a study on nuclear reactors, Ghosh and Wilson [18] suggested that the width and depth of the soil deposit should be at least 3 and 1.5 times the width of the building, respectively. Paultre and Lavoie [19] also recommended that the soil deposit be 3 times larger than the building. Lysmer and Kuhlemeyer [20] and Wilson [21] showed that using non-reflecting radiative boundaries allows one to reduce the size of the soil deposit without affecting the structural behaviour. Those boundary elements are viscous dampers with a value per surface unit of $\rho_s V_s$, where V_s is the shear wave velocity in the soil medium and ρ_s is the soil density.

(3) As explained, seismic waves are modified by the mass and stiffness of the soil and also by the interactions with the structure and its foundation. However, available ground motions are often signals recorded on the surface, called free-field motions. Thus, particular care should be taken regarding the input mechanism for these signals [16]. The three possible input mechanisms studied in Léger and Boughoufalah [22] are described in the following subsections.

3.1.1. Massless foundation

This input mechanism implies that one should define the mass of the soil elements as null. In this way, the signal can be input at the base of the soil deposit because seismic waves do not undergo any modifications by propagating in the soil medium. Using the free-field ground motions is then acceptable, as the motions that reach the surface are the same as the one input at the bottom. In this mechanism, soil elements are modelled only for their flexibility; their inertia is neglected.

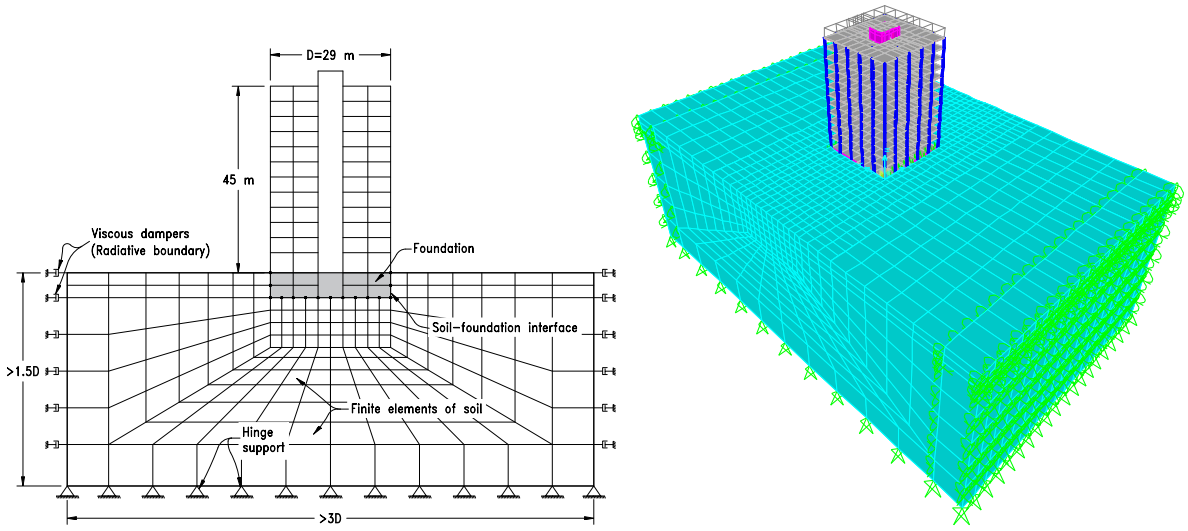

Figure 2: Direct method for modelling SSI, (a) conceptual model (b) 3D model in SAP2000. [Colour online].

3.1.2. Surface input

The surface input mechanism consists of inputting the free- eld ground motion directly at the surface of the soil deposit. To this end, the acceleration signal of the ground motion is applied to all joints of the soil-foundation interface. The implementation of this mechanism in modelling software requires care. It is important that the mass degrees of freedom of the soil be identi ed so that the loading is not applied to them [21].

3.1.3. Deconvolution

A more realistic excitation of the structure can be obtained by computing a motion at the base of the soil deposit that could have caused the free- eld motion. This process is called deconvolution. Many software packages, such as SHAKE[23] and DEEPSOIL[24], are available to solve this complex mathematical problem. However, such software packages are quite cumbersome and sensitive to input parameters. Another approach is to solve the wave propagation problem directly in the nite element model, eliminating possible mistakes [25].

The deconvolution in this project is performed by applying the free- eld motion at the base of the soil deposit and then recording the acceleration at the surface in the nite element model without the aboveground structure. Correction factors are then computed by comparing the recorded signal to the free- eld target motion in the frequency domain. Finally, these factors are applied to the original signal in the frequency domain. This method is derived from the mathematical formulations of Meimer[26], by which it is possible to demonstrate the accuracy of the procedure for a completely linear system. Otherwise, the process is generally repeated until the results are satisfactory.

3.2. Substructure method

Substructure method is an equivalent approach to model SSI. Theoretically, this method splits the problem in two distinct parts that are solved separately. The first part consists in calculating the free-field motions or the foundation input motions without considering the presence of the structure. In practice, this part is often not necessary, because soil dependant free-field ground motions are directly available. The second part consists in applying the motion to the structure in which soil properties are simulated by a group of equivalent springs and dashpots. Because of the superposition inherent in this method, the soil and the structure need to be assumed linear. However, an equivalent linear system is often used to respect that criterion [16].

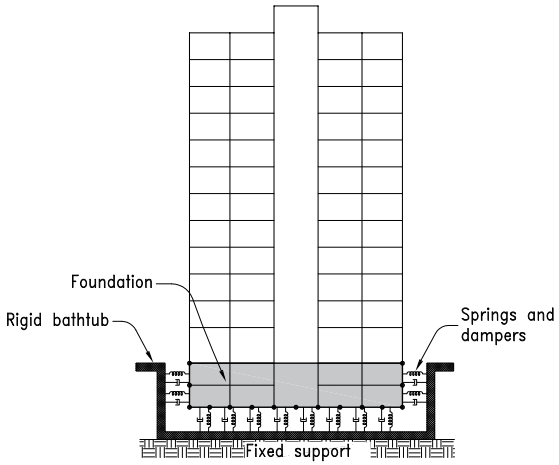

Figure 3: Substructure method for modelling SSI using the bathtub approach.

Multiple variants of modelling SSI with the substructure method exist. Some such variants have been compared in NIST GCR 12-917-21 [16]. The main differences in these approaches concern the seismic input motion mechanism. One of these approaches is called the bathtub approach (fig. 3). The same signal is applied to all springs and dashpots through a rigid "bathtub". Another approach is to consider the variation of the signal over the depth of the foundation. Though the latter is more precise, it is difficult to model.

The substructure method requires the computation of equivalent soil properties that are assigned to each spring and dashpot. Soil dynamic properties, known as impedance functions, depend on the foundation geometry, the nature of the soil as well as the excitation frequencies. The derivation of the impedance functions is very challenging. Thus, equations for simple cases of foundations laying on a linear homogeneous half space are proposed in Pais and Kausel [27], Gazetas [28] and Mylonakis et al. [29], which are recommended in NIST GCR 12-917-21. The equations proposed by Pais and Kausel [27] have also been included in the latest edition of ASCE 7-16 [1].

4. Studied methods

In this paper, two methods are studied to consider foundation movements. They are labelled SS and RO and are described in the next paragraphs. The demands in the elements part of the GLRS are then determined according to the procedure proposed by Beauchamp et al. [10] on a model that incorporates one or the other of the studied methods. In this way, foundation movements can be considered in the calculations.

The first method studied in this paper is labelled SS to indicate substructure. It consists of adding springs and dashpots based on the bathtub approach of the substructure method described in section 3.2. The model corresponding to the SS method is shown in Fig. 4. This model has been developed for a concrete building with isolated footings under cores and columns but can be modified for other configurations. At the surface, the soil is often not strongly compacted to offer a passive lateral resistance; thus, horizontal springs and dashpots are not assigned at the ground level. Simple impedance functions to calculate springs and dashpots are based on the hypothesis that the foundation acts as a whole. However, walls and columns are often on isolated footings that allow them to rotate independently. Thus, joints at the base of the foundation are constrained by a rigid diaphragm only. To simulate the rotational stiffness when uniaxial springs are distributed under the foundation, NIST GCR 12-917-21 [7] proposes simple equations to increase the stiffness of the springs on a strip along the foundation edges. However, this approach neglects the important rotational stiffness of the core footing. To solve that problem, all joints under the core are constrained to act as a "rigid plate", and a rotational spring is added as shown in Fig. 4. It has been found that moment demand on the column footings is small in regard to their capacity, leading to almost no rotation. Thus, the rotational degrees of freedom (DOFs) at the base of the columns and the out-of-plane rotational DOF at the base of the foundation walls are restrained. This simplification may not be adequate for all buildings, and verification is necessary.

The RO method is studied to further simplify the calculations (Fig. 4). Basically, this method consists of adding a single rotational spring under the core. All other joints under the foundation are fully restrained. As described for the SS method, all joints under the core are constrained to act as a "rigid plate" that is connected to the rotational spring.

4.1. Calculation of springs and dashpots

Springs and dashpots are computed according to the procedure given in NIST GCR 12-917-21 [7], which is based on the impedance functions proposed by Pais and Kausel [27]. Global stiffness and damping values of the whole foundation are first computed and then transferred into a set of uniaxial springs and dashpots. To do so, the vertical stiffness and damping are distributed to the vertical springs and dashpots according to their geometrical tributary area. The rotational stiffness and damping are then considered by increasing the values of springs and dashpots on a strip along the foundation edges according to simple equations proposed in NIST GCR 12-917-21 [7]. The horizontal stiffness and damping resulting from the passive lateral resistance of the soil are distributed to the horizontal springs and dashpots according to their geometrical tributary area. Part of the horizontal stiffness and damping resulting from other effects are equally distributed to the horizontal springs and dashpots at the base only.

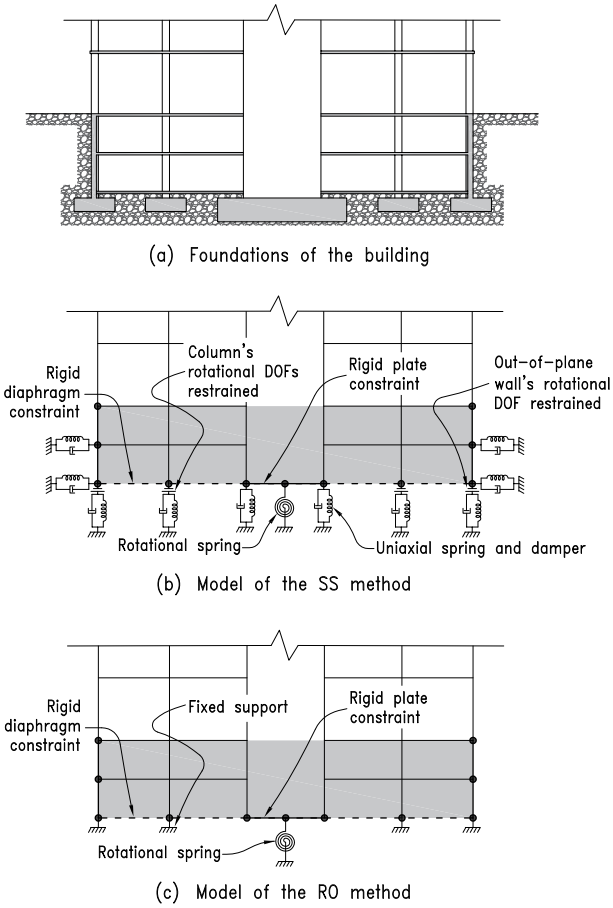

Figure 4: Illustration of the studied methods.

The added rotational spring stiffness can be evaluated following the same procedure with the dimensions of the core footing only. Another simple approach is to evaluate this stiffness as a ratio of the square of the core footing length to the square of the total foundation length. This rotational spring stiffness is then subtracted from the global foundation rotational stiffness. The rotational stiffness of the core footing can also be evaluated using Eq. 1 given in CSA A23.3-14. In this case, the stiffness is simply the applied moment over the rotation calculated. The refined procedure developed by Adebar [15] can be used for that purpose as well.

For this project, rotational spring in the model SS has been computed by the lengths ratio because of the simplicity of this approach. On the other hand, in the model RO, the spring has been computed following the procedure in NIST GCR 12-917-21 with the core footing dimensions.

4.2. Performance of SSI models

As discussed in Section 4, the SS method differs from the basic substructure procedure given in NIST GCR 12-917-21 [16] because of the added rotational spring. Thus, as the direct method is the most rigorous approach to modelling SSI, it is used to assess the performance of the SS and the RO method for linear homogeneous soil

media. A complete linear 3D model of the soil-foundation-structure system has been modelled, as shown in Fig. 2, in the SAP2000 software package [30]. Because the depth of the soil deposit is more than 1.5 times the width of the building, fixed conditions are assumed at the base without significantly affecting the behaviour of the structure [18]. However, radiative viscous boundaries are assigned to the sides of the deposit to ensure that horizontal shear waves are not reflected back to the structure [20, 21]. Verification has been performed to ensure that the four corners of the building, in a model with only the soil deposit and the flat box foundation, are seeing the target free-field motion when the deconvolved signal is applied at the base of the deposit.

The direct method is modelled with each of the three input mechanisms discussed in Section 3.1: (1) deconvolution, (2) surface input, and (3) massless foundation. The reference method is the deconvolution, as it considers all SSI effects. Comparisons are made for a class D soil ($V_{s,30}$ = 250 m/s) using a single unscaled seismic record. For each input mechanism, the envelope of the shear demand in the core and the envelope of the interstorey drift ratios have been extracted (Fig. 5). The SS method results are in good agreement with the analyses performed with the reference solution. For this building subjected to horizontal excitations, the three seismic input mechanisms produced similar results (Fig. 5). The RO method also achieves good results for aboveground storeys, although it overestimates the shear demand in the core for underground storeys. Based on these observations, it is determined that the SS approach is an efficient way to model SSI for the studied building. The SS method will be carried forward in NLTHA to consider SSI in the most realistic manner for this study. The RO method will still be analysed in linear models considering the simplicity of its implementation.

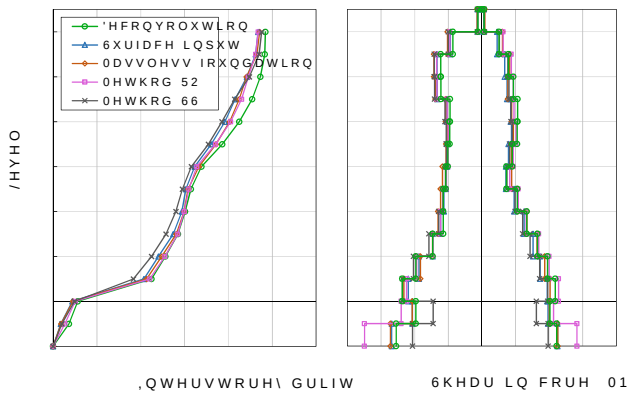

Figure 5: Comparison of the different methods for modelling SSI. [Colour online].

5. Application of proposed methods

As described in Section 4, two methods for considering foundation movements are studied in this paper. The first method, labelled SS, is a complete set of springs and dashpots, as shown in Fig. 4b. The other method is labelled RO and consists of a single rotational spring under the core, as shown in Fig. 4c. To verify the influence of SSI, a fixed-base model including the underground storeys is also studied and labelled FB. For all these models, the forces

in elements part of the GLRS are determined with the method proposed in Beauchamp et al. [10], as described in Section 2.3. This method can be applied directly to the finite element model of the building, labelled GNS, or with a stiffness reduction in the plastic hinge zone, labelled GNS_LPH. Thus, globally, 5 original models are studied and analysed: GNS_LPH_FIX, GNS_SS, GNS_RO, GNS_LPH_SS and GNS_LPH_RO. The meanings of the acronyms in the model names are summarized in Table 1. The fixed-base model is studied only with a stiffness reduction in the plastic hinge zone to lighten the figures and because it was shown to be more precise in Beauchamp et al. [10]. In addition, the forces in elements part of the GLRS are computed according to the method proposed in CSA A23.3-14 and described in Section 2.2 for comparison. This curve is labelled CSA.

To assess the performance of the models, NLTHA is performed for each case to serve as target values. The purpose of NLTHA is to be as close as possible to reality. Thus, in these analyses, SSI is modelled according to the SS method discussed in Section 4.2.

The influence of SSI is verified by performing all the analyses for three types of soil with an uncracked underground structure. Analyses are also performed with a severely cracked underground structure to study the effect of this parameter. An explanation of the underground structure cracking level is given in Section 5.2.

Table 1: Description of acronyms used in model names

Acronym	Description
SS	Sub-Structure: SSI modelled with the SS method
RO	Rotational spring Only: SSI considered via a rotational spring under the core only
FIX	FIXed: Fixed-base model including the underground storeys
LPH	Linear Plastic Hinge: Stiffness reduction over the plastic hinge zone
GNS	Gravity nearly Null Stiffness: Stiffness reduction in the GLRS for RSA analysis

5.1. Studied building

The studied building (Fig. 6) is one of the buildings presented in the seismic design chapter of the Concrete Design Handbook [14] to illustrate the use of seismic design regulations for reinforced concrete structures. It was also used in the paper in Beauchamp et al. [10]. This building, located in Montreal, has two underground storeys. The SFRS consists of one core made up of two C-shaped walls connected by coupling beams. These C-shaped walls behave as cantilever walls in the North-South direction and as coupled walls in the East-West direction; therefore, both of these two types of SFRS can be studied.

According to the Concrete Design Handbook [14], the building has been designed with force reduction factors related to ductility and overstrength of $R_d = 3.5$ and $R_o = 1.6$, respectively, in the cantilever wall direction and $R_d = 4.0$ and $R_o = 1.7$ in the coupled wall direction, respectively, as defined by the NBCC 2015 [21]. The seismic design of the SFRS has been performed for a class D soil according to the NBCC 2015 and CSA A23.3-14 [

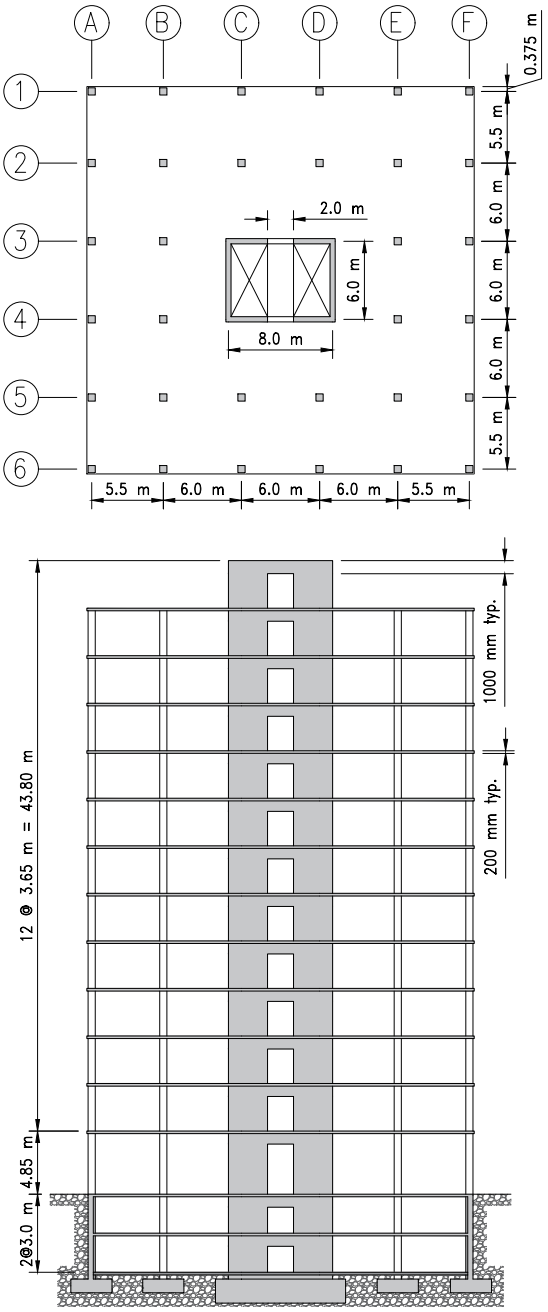

Figure 6: Plan and elevation of the studied building adapted from [104]

The seismic forces have been computed with the response spectrum method on a fixed-base model including the underground storeys. The design base shear has been scaled at the ground level because the shear distribution of the lateral earthquake force computed according to the equivalent static procedure does not consider underground storeys [2]. The flexural reinforcement of one C-shaped wall is presented in Fig. The plastic hinge zone has

been determined to extend over the first three storeys above ground. According to the capacity design principle, reinforcement in walls under the ground level has been increased to ensure that yielding does occur in the plastic hinge zone. Hence, flexural concentrated reinforcement bars have been upgraded from 25M to 30M in the underground storeys.

In this paper, the building is analyzed on three different soil classes. Thus, the seismic design of the SFRS have also been performed for class C and E soils. As the design is governed by the minimum steel requirements, the same reinforcement is used for all three soil classes.

All the aboveground structural elements have been modelled with cracked section properties as recommended in CSA 23.3-14 (Table 2). For the design of the GLRS, an upper bound estimate of these cracked section properties should be used. Beauchamp et al. [10] suggested that the effective properties all be increased by 25%. However, because the stiffness reduction factor is constant for all members, the force in these members would simply be 25% larger. Hence, the distributions with the upper bound estimation are not presented in this paper to avoid over-crowded figures.

Table 2: Cracked section properties for linear analysis.

Element type	Effective properties
Columns	$I_e = 0.55I_g$ to $0.65I_g$
Coupling beam	$A_{ve} = 0.45A_g$; $I_e = 0.25I_g$
Slab frame element	$I_e = 0.2I_g$
Wall (soil C)	$A_{xe} = 0.65A_g$; $I_e = 0.65I_g$
Wall (soil D & E)	$A_{xe} = 0.5A_g$; $I_e = 0.5I_g$

5.2. Modelling of underground storeys

Buildings generally have underground storeys that are much stiffer than the remainder of the building because of the long perimeter walls. Lateral forces from the SFRS are partly transferred to these perimeter walls by the diaphragms formed by floor slabs. This is known as backstay effect. Explicitly modelling the underground storeys is important to obtain a more realistic behaviour of the building during an earthquake. This has been done for all models of this study. The design of the aboveground part of the SFRS is generally safely made with the uncracked section properties of the underground structure. Indeed, this model is the most rigid which means it has a shorter period and produces the largest seismic forces in the shear walls at the ground level. On the other hand, there is a great uncertainty in the properties of structural components in underground storeys. Thus, it is recommended that these properties be bracketed to capture the most critical behaviour of all structural elements of the underground storeys [31].

To be consistent with the design of the aboveground part of the SFRS, all analyses in this paper are performed considering uncracked properties of the underground structure to determine seismic forces in the aboveground elements

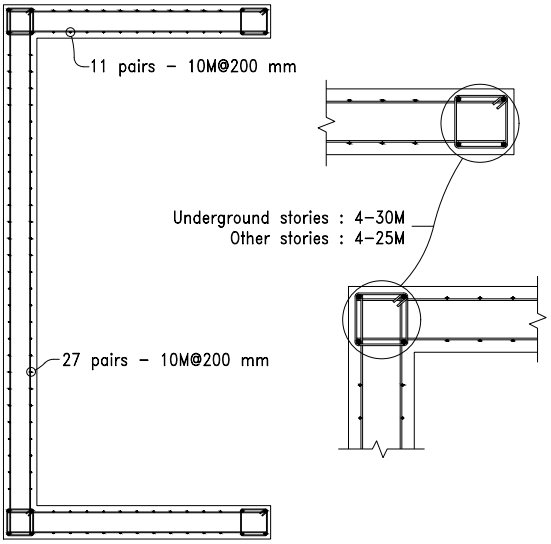

Figure 7: Detailing of exural reinforcement in walls.

part of the GLRS. However, the cracked section properties of the underground structure may increase the displacements of the building and thus the forces in the GLRS. Therefore, analyses are performed with severely cracked section properties of the underground structure to study this e ect. The severely cracked properties have been determined using the lower bound recommendations in PAEER 2012 72-1 [31] (Table 3). To e ectively model the stiness of the oor slabs, semi-rigid diaphragms are assigned for underground storeys.

Herein, the soil supporting the underground storeys is represented by the exibility of an equivalent linear elastic medium according to the current sate-of-the-practice, (Figs 4b,c) (34). However one should be aware that Fatahi and Tabatabaiefar [32] have shown that depending on the nonlinear characteristics of the subsoil de ned by the plasticity index, it is possible that for mid-rise building frames resting on soft soil deposits, the base shears increase, while the lateral de ections and corresponding interstorey drifts decrease.

Table 3: Sti ness considered for severely cracked properties of underground storeys.

Sti ness of core walls	$0.8E_cI_g$
Shear sti ness of diaphragms	$0.05G_cA_v$
Shear sti ness of foundation walls	$1.0G_cA_v$
Flexural sti ness of diaphragms	$0.2E_cI_g$
Flexural sti ness of foundation walls	$0.2E_cI_g$

5.3. Soil parameters

The influence of SSI is verified for soil classes C, D and E according to NBCC 2015 [2] and ASCE 7-16 [1]. For all cases, the soil is considered as a linear homogeneous half space. The properties of every type of soil are described in Table 4 along with the key parameters used in the analyses. The shear wave velocities are taken according to the NBCC 2015 values for each soil class [2]. The values of the soil hysteretic damping ratio (ξ_s) and effective soil modulus ratio (G/G_0) are taken from tables proposed in Chapter 19 of ASCE 7-16 [1]. The maximum shear modulus of the soil at small strain levels (G_0) is calculated according to

$$G_0 = \rho_{soil} V_{s30}^2 \tag{3}$$

The other soil parameters are average values taken from the literature and experience.

Table 4: Summary of studied cases along with their key parameters.

No.	Soil	Found.[1]	Direction	T_1^2 (s)	$S(T_1)^2$ (g)	ξ_s -	$\xi_{Rayleigh}$ -	G/G_0 -	V_{s30} (m/s)	ρ_{soil} (kg/m^3)	G_0 (kPa)	-
1	C	UNCR	Coupled	1.89	0.077	1.39%	2%	0.91	450	2000	405000	0.33
2	C	CR	Coupled	1.95	0.072							
3	C	UNCR	Cantilever	2.21	0.065							
4	C	CR	Cantilever	2.27	0.064							
5	D	UNCR	Coupled	1.96	0.096	2.98%	2%	0.82	250	1900	118750	
6	D	CR	Coupled	2.06	0.091							
7	D	UNCR	Cantilever	2.27	0.086							
8	D	CR	Cantilever	2.39	0.084							
9	E	UNCR	Coupled	2.34	0.120	8.30%	2%	0.48	115	1800	23805	
10	E	CR	Coupled	2.72	0.108							
11	E	UNCR	Cantilever	2.58	0.112							
12	E	CR	Cantilever	3.08	0.097							

[1] UNCR : uncracked underground structure; CR : Severely cracked underground structure

[2] Calculated with SS model and effective section properties according to CSA A23.3-14

Tabatabaiefar et al. [33], performed extensive 2D parametric analyses of the seismic demand on moment frame buildings including SSI with a mass foundation model and absorbing boundaries using the FLAC computer program [34]. Soil site classes C, D and E were considered with nonlinear stress-strain soil models [35, 36]. It was shown that it is essential to consider SSI for soil classes D and E to assess adequately the frame displacements and internal forces. These findings were corroborated from shake table experiments on small scale frame models by Tabatabaiefar

and Clifton [36]. Simplified modelling procedures using linear soil behaviour were also studied by Tabatabaiefar and Massumi [37] leading to similar conclusions. However, modelling and simulations of nonlinear soil behaviour are complex to validate and beyond the scope of the state-of-the-practice as noted in the latest guidelines from the Los Angeles Tall Buildings Structural Design Council (LATBSCD) [38]. The LATBSCD recommends for practical SSI modeling the bathtub model (Fig. 3) or the use of interaction elements at the foundation level only, which correspond the SS (Fig. 4b) or RO (Fig. 4c) methods studied herein.

5.4. Finite elements modelling strategy

The approach in this paper is to apply the methods as would be done in an engineering office. To this end, all linear analyses are performed with the SAP2000 software [30]. In SAP2000, columns are modelled with frame elements, while core walls, foundation walls, slabs and coupling beams are modelled with shell elements. In linear analyses, the SS, RO and FIX methods are investigated to consider foundation movements. These methods are summarized in Table 1. The nonlinear analyses are performed with SeismoStruct [39], which offers a user-friendly interface and a large range of uniaxial material laws for fibre-based elements. To determine seismic forces in the GLRS, CSA A23.3-14 simply requires that "the inelastic displacement profile of the SFRS shall be accounted for." [6]. Hence, only the SFRS is modelled with nonlinear elements; all other structural components are modelled with elastic frame elements. NLTHAs are meant to be as realistic as possible; therefore, the SSI is modelled with a set of springs and dashpots according to the SS method discussed in Section 4.2.

In SeismoStruct, the cores walls are modelled with C-shaped nonlinear fibre-based elements. Thus, each section of the C-shaped walls has only one control node, which has been proven to increase the stability of the model. The coupling beams are modelled with elastic beams and nonlinear flexural springs, as suggested by Naish et al. [40]. The initial effective stiffness of the coupling beams is calculated according to Spacone Vu et al. [41]. The conceptual approach to modelling walls and coupling beams is shown in Fig. 8.

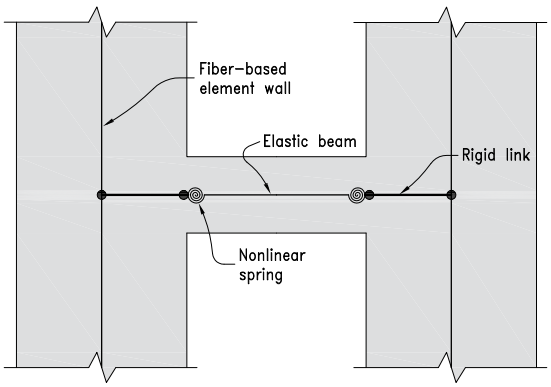

Figure 8: Nonlinear modelling approach of walls and coupling beams.

All concrete in the building has a compressive strength of 30 MPa. Thus, Young's modulus is assumed to be $E_c = 25000$ MPa for all elements in linear analyses. In nonlinear analyses, the concrete is defined by the constant

con nement model proposed by Mander et al. [42]. For reinforcing steel, the model based on the relationship proposed by Menegetto and Pinto [43] is chosen. As implemented, this model also includes the isotropic hardening rules proposed by Filippou et al. [44]. This model is suggested in the SeismoStruct User Manual for reinforced concrete elements subjected to complex loading histories [45]. The parameters for the concrete are adjusted to represent a 30 MPa compressive strength and 3.11 MPa tensile strength. For reinforcing steel, the parameters are adjusted to represent a 400 MPa yield strength and a strain hardening ratio of 0.005.0

5.5. P-Delta e ects

Particular care should be taken when activating the P-Delta option in nite element software when using the proposed method to determine the seismic demands in the GLRS. Because the stiness of the columns is greatly reduced, the negative terms in the geometric matrix (which depends on the axial load and the length of the column) could be larger than the actual terms in the stiness matrix of the element. This means that an unwanted negative term may appear in the global stiness matrix, leading to local instability and possible convergence problems. P-Delta options in which the structure is treated as a simpli ed stick model, as in the iterative based on mass option in the ETABS software [46], can be used without issue, as the stiness of the walls ensures the stability of the model.

5.6. Gravity load and damping

Contrary to linear analyses, nonlinear analyses are load path dependent. Indeed, the neutral axis position in sections of bre-based elements depends on a combination of the moment and the axial load. Thus, the speci ed mass needs to correspond to the expected mass and not to the factored gravity loads. In this project, the gravity load in NLTHA is taken as the seismic mass recommended in NBCC 2015 [2], which is a part of the live load as recommended in PEER/ATC 72-1 [31]. The seismic mass is then computed as

$$1.0D + 0.25S + 0.4 \quad 0.5L = 1.0\,\text{Dead} + 0.25\,\text{Snow} + 0.2\,\text{Live} \tag{4}$$

For NLTHA, part of the damping is inherent to the hysteretic behaviour of nonlinear materials. Other sources of energy dissipation that are not explicitly modelled can be included via viscous damping. However, there is no clear agreement on how to model this viscous damping [45]. [PEER/ATC 72-1 [31] compared di erent methods, and Rayleigh damping, proportional to the mass matrix and the tangent stiness matrix, achieved the best results for maintaining a given level of damping when the fundamental period of the building lengthens. Thus, for NLTHA, Rayleigh damping proportional to the mass matrix and the tangent stiness matrix with a critical damping ratio of = 2% is speci ed. The constants are computed with the rst and last mode required to obtain 90% of the e ective modal mass. For linear analyses, a constant damping ratio of 5% for all modes is speci ed.

6. Ground motion selection

Because every earthquake is di erent, NLTHA requires the selection of multiple ground motions to obtain a realistic response of the structure. This response may correspond to the mean behaviour of all selected motions. In

this project, each of the 12 cases (Table 4) is analysed with 16 ground motions selected from the conditional spectrum (CS) method. Globally, 6 different sets of 16 ground motions are selected, as the 2 levels of cracked underground structure are analysed with the same set of ground motions.

All selected motions need to be scaled to a defined intensity level. In this project, the target intensity level corresponds to an earthquake with a probability of exceedance of 2% in 50 years, which is the design intensity level defined in NBCC 2015 [2]. For this intensity level, the NBCC gives the values of the maximum acceleration of a structure of variable period via uniform hazard spectrum (UHS). Thus, ground motions are selected such that the maximum acceleration of the structure corresponds to the spectral acceleration prescribed in NBCC 2015. However, selecting ground motions that are generally equal to the UHS for all periods is not realistic because the UHS are defined from many records and ensure the same probability of exceedance for all periods. Baker [47] showed that using motions scaled to the UHS is too conservative and thus proposed an approach based on the conditional mean spectrum (CMS). Because NLTHAs are aimed at being as close as possible to reality, the latter approach is preferred, as the selected ground motions are more representative and consistent for a given intensity level [47].

6.1. Conditional spectrum method

The CMS is the expected spectrum, consistent with the probabilistic seismic hazard analysis (PSHA), conditioned to reach a target spectral value at the period of interest T_{int} [47]. The conditional spectrum (CS) method is an extension of the CMS that considers the variability of spectral amplitudes at periods other than T_{int}. It ensures that spectral accelerations of the selected motions, at high and low frequencies, are correctly scattered to obtain a representative envelope of the response. Recently, Baker and Lee [48] proposed an efficient CS method algorithm based on MATLAB [49]. This algorithm, with a few adaptations to consider the Eastern North America region, is used in the current project. An example of a set of selected motions is shown in Fig. 9.

In this project, the period of interest corresponds to the first lateral period (T_1) of the cracked structure, including the flexibility of the soil. Indeed, for concrete wall structures, the demands in the GLRS depend on the interstorey drift, and this parameter is mainly controlled by the first vibration mode [8]. The range in which the variability of the selected motions is conditioned to the CMS is approximately $0.5T_1$ to $2.0T_1$. Because the same set of ground motions is used for the cracked two levels of underground structure, the period of interest is taken as the mean of the first lateral period of these two cases. These periods and their target spectral values are presented in Table 4.

To apply the CS method, a mean representative event of the seismic hazard is needed. Because seismic hazard maps in Canada are computed by a PSHA, this event is determined by a disaggregation of the seismic hazard in Montreal with the OpenQuake software [50]. This results in an event defined by a magnitude M, a distance R and a variable $\varepsilon(T)$. The last variable represents the number of standard deviations ($\sigma_{\ln S_a}(T)$) between the logarithm of the spectral response at T ($\ln S_a(T)$) and the mean prediction of the response for the couple (M, R) ($\mu_{\ln S_a}(M, R, T)$). To be consistent with the intensity level of the NBCC 2015, the spectral ordinate at the CMS is forced to correspond to the value of the UHS NBCC 2015 spectrum. Then, $\varepsilon(T_{int})$ is back calculated in the process according to

the following equation:

$$\ln S_a(T) = \ln S_a(T) \qquad \ln S_a(M;R;T) = \ln S_a(T) \tag{5}$$

In the process described above, the prediction of the response corresponding to a specific event is obtained using ground motion prediction equations (GMPEs). To be consistent, the GMPEs used to develop the NBCC 2015 seismic hazard maps are used. These GMPEs are implemented in the algorithm in the form of look-up tables that are based on Atkinson and Adams [51]. Shallow crustal earthquakes are the main type of events expected in Eastern North America (ENA) [52]. Thus, only one set of GMPEs is needed. This set is divided into a lower, central and upper GMPE that are used through a logic tree. This approach is a simple and efficient way to represented epistemic uncertainty [51].

The availability of strong ground motion records is very limited in ENA; thus, the records have been selected from the PEER NGA-West2 database [53]. Because the attenuation of the ground motions in ENA is different than in WNA at low periods, this approach may be inadequate. However, if the spectral shape of the selected records well match the CMS developed for ENA, the selected ground motions may be acceptable [52].

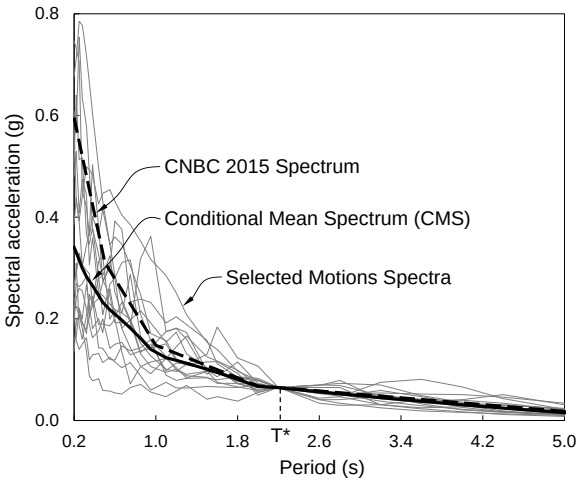

Figure 9: Example of selected ground motions for soil C in the coupled walls direction ($T = 2.24$ s).

6.2. Considering soil class

GMPEs look-up tables have been originally developed for a soil class B (Class C according to NBCC 2015 classification) and then converted for a soil class C as described in Atkinson et al. [54]. In this project, multiple soil classes are studied; therefore, GMPEs need to be converted accordingly. Based on the tables for a soil class C, values of the response at the building location could be converted using the site modification factors of NBCC 2015 art. 4.1.8.4 [2] that depend on the peak ground acceleration, the period and the soil class. These factors are based on the GMPE proposed by Boore and Atkinson [55] which follows a procedure developed by Choi and Stewart [56]. Indeed, target spectrum at the period of interest is also modified to take account of the soil class with the same factors.

7. Analyses results

In Figs. 10 to 15, the results for the uncracked section properties of the underground structure are presented to compare the in uences of the soil type. From left to right, the results are presented for soil classes C to E. The upper and lower rows concern the cantilever and the coupled wall direction, respectively. In each gure, all models are compared to the reference curve (NLTHA) for one parameter. The interstorey drift is presented for the two directions in Figs. 10 and 11. Two types of columns are then analysed. Corner and interior columns present quite di erent behaviours, as the latter extends in the underground storeys and the former extends in the rigid foundation walls. The envelopes of the absolute exural moment are presented for both types of columns. Figs. 12 and 13 present the results for a corner column (column F6 in Fig. 6), while Figs. 14 and 15 present the results for an interior column (column C5 in the cantilever wall direction and E3 in the coupled wall direction in Fig. 6). Shear envelopes are not presented to limit the number of gures. However, the distribution of the shear is similar to that of the exural moment, and the same observations would have been made.

The e ect of a severely cracked underground structure is analysed in Figs. 16 to 18. These gures present the interstorey drift and exural moment in the corner column F6 and middle column C5 in the cantilever wall direction.

The model names and characteristics are described in Section 5. However, the GNS label preceding the LPH label in the model names has been removed in the gure legends to avoid having an oversized legend box.

7.1. Nonlinear time history analyses

In total, 192 NLTHAs were performed. The curve labelled NLTHA corresponds to the mean response of the 16 ground motions selected for one case. A typical representation of the variation of the results is represented by a shaded area that corresponds to 1 standard deviation ( ). As discussed, NLTHA is the most rigorous analysis method used in this project. The inelastic displacement pro le is directly considered, and the SSI is modelled with a set of springs and dashpots according to the SS method, as discussed in Section 4.2. Therefore, its results are used to evaluate the performance of the other simpli ed methods, and the shaded area de nes the target values.

NLTHA captures the inelastic behaviour of the SFRS that is generally concentrated at the base of the walls over the height of the plastic hinge zone. As the seismic excitation increases (from soil classes C to E), higher nonlinearity is observed, and the variation in the results decreases. This is clear in all gures (Figs. 10 to 18) and can be explained by the capacity design principle. If the wall severely yields for all ground motions, the seismic force developed in the SFRS is somewhat limited and is the same for all seismic input records.

7.2. In uence of soil class

For the interstorey drift (Figs. 10 and 11), as was expected, the exibility of the foundations has almost no e ects for a sti soil, whereas it becomes more important as the soil becomes softer. For soil class C, the SS, RO and FIX models give almost the same results. The response is more strongly in uenced by the stress in the plastic hinge zone, and the linear plastic hinge (LPH) approximation leads to accurate results compared to NLTHA. As the soil

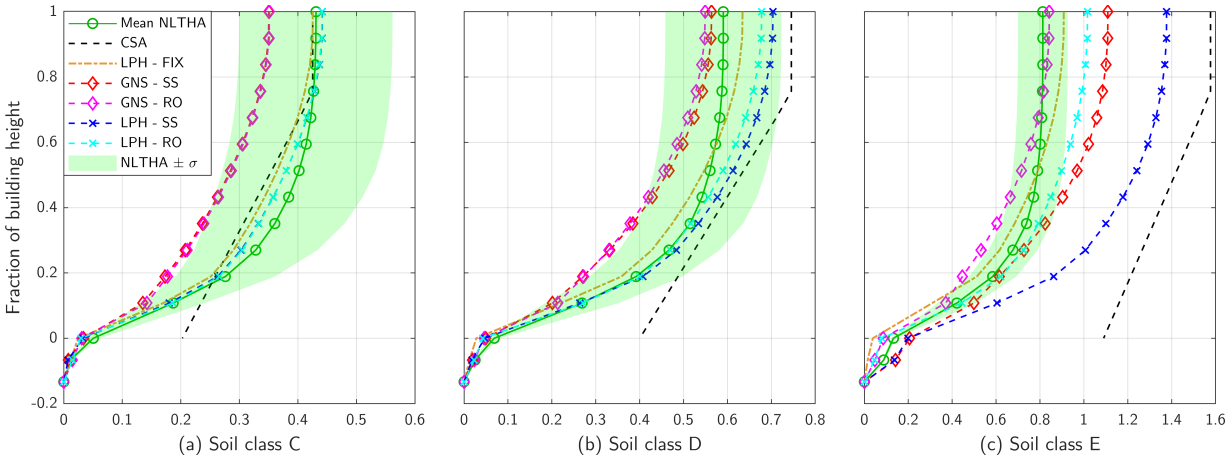

Figure 10: Lateral interstorey drift ratio, in percentage, for the cantilever wall direction with uncracked section properties of the underground structure. [Colour online].

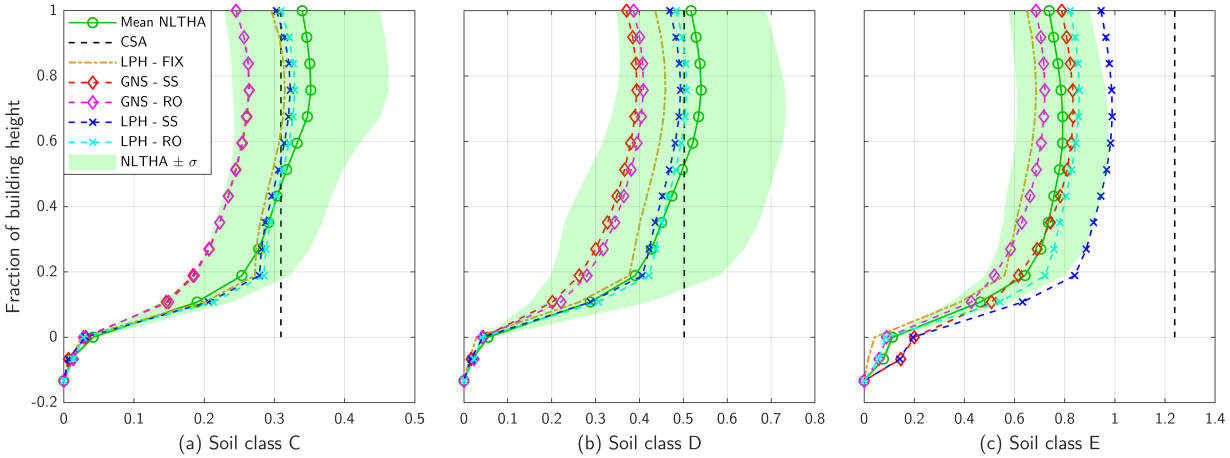

Figure 11: Lateral interstorey drift ratio, in percentage, for the coupled wall direction with uncracked section properties of the underground structure. [Colour online].

becomes softer, for soil class E, the SS and RO models tend to overestimate the interstorey drift. Only the xed-based model (LPH_FIX) remains in the target range for all cases, always being slightly lower than or crossing the NLTHA curve. These curves show that reducing the stiffness of the walls in the plastic hinge zone (LPH models) is the most important parameter in not underestimating the interstorey drift. The LPH_RO and LPH_FIX curves are generally the best t for all cases compared to NLTHA. The simpli ed method in CSA A23.3-14 (curve CSA) globally well de nes the shape of the interstorey drift pro le. However, it slightly underestimates the demands for soil class C and largely overestimates it for soil class E. The relevance of the curve for coupled walls introduced in the Explanatory Notes on CSA A23.3-14 and highlighted rst by Beauchamp et al. [10] is clearly shown in Fig. 11.

For the exural moment in the corner column (Figs. 12 and 13), all models are equivalent for the upper storeys. They are accurate compared to the NLTHA curve for almost all cases, except for soil classes C and D in the cou-

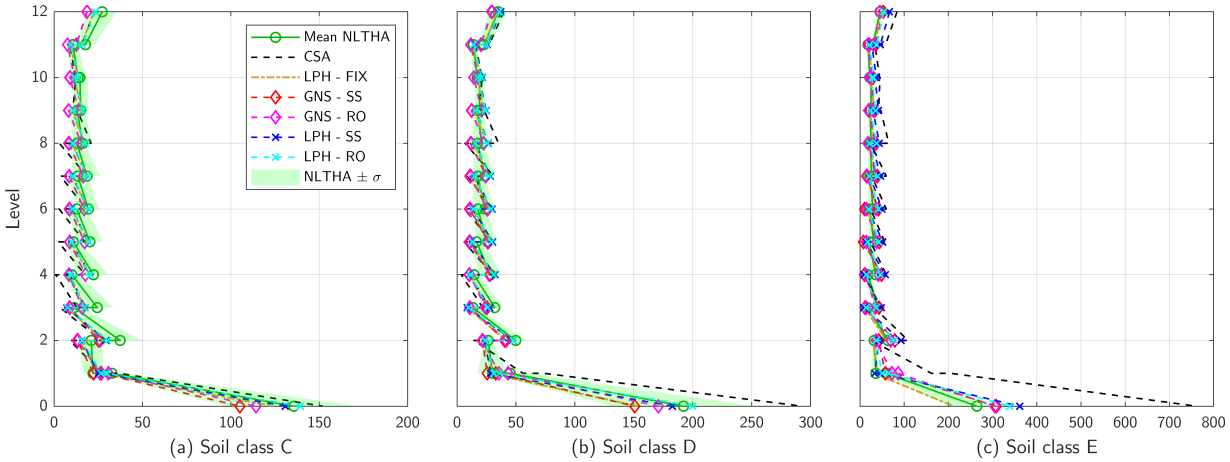

Figure 12: Flexural moment, in kNm, in column F6 for the cantilever wall direction with uncracked section properties of the underground structure. [Colour online].

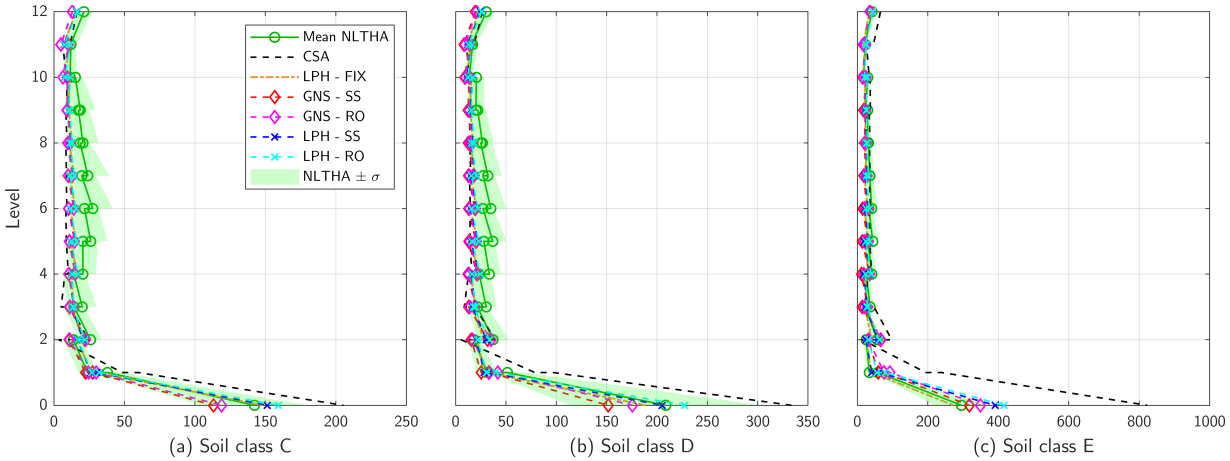

Figure 13: Flexural moment, in kNm, in column F6 for the coupled wall direction with uncracked section properties of the underground structure. [Colour online].

pled wall direction (Figs 13a and 13b), where the demands are a lower bound estimate. For the lower storeys, and particularly at the base, greater variability is observed from one model to the next. For soil classes C and D, the LPH_RO and LPH_SS models give an upper bound estimate, while the GNS models give a lower bound estimate. LPH_FIX is also accurate for soil class C but slightly underestimates the demands for soil class D and overestimates for soil class E. This could be expected, as SSI has stronger effects when the soil becomes softer. For soil class E, all models expect LPH_FIX are upper bound estimates. For all cases, modelling the foundation movements with a single rotational spring (RO) leads to higher demands at the base than when SSI is modelled with a complete set of springs and dashpots (SS). LPH_SS is more accurate than NLTHA, while LPH_RO is an upper bound estimate.

For the flexural moment in the interior column (Figs 14 and 15), greater dispersion is observed in the upper storeys. For soil classes C and D, all models are a lower bound estimate, with the GNS_RO and GNS_SS models

being outside of the target range. For soil class E, all models are rather an upper bound estimate, except for LPH_FIX, which is still a lower bound. At the ground level, the same observations described above for the corner column can be made. In the underground storeys, as could be expected, the LPH approximation no longer holds, as the reduction in the plastic hinge is aboveground. The behaviour is more strongly influenced by the method for modelling foundation movements. The SS models give the best results compared to NLTHA, while the FIX model does not capture the behaviour of the underground column, particularly on soft soil.

In contrast to the insterstorey drift, the flexural moment in the columns is better estimated with SS models in which foundation movements are considered by the more detailed method. This is especially true for columns in the underground levels. However, using a single rotational spring leads to pretty good results considering the simplicity of its implementation. The LPH_FIX model, which ignores foundation movements, is surprisingly a good lower bound estimate, even for soil class E. However, ignoring foundation movements leads to a poor estimate of demands in underground columns.

For the CSA method, the interstorey drift curves in Figs. 9 and 11 show an important initial drift at the ground level. However, in regard to imposing this displacement profile onto the building, the method does not hint at how to consider the initial drift in the underground storeys. Displacing the ground level to this drift value relative to the base is not realistic because unreasonable forces and deformations occur in foundation walls. Thus, in this paper, zero-displacement conditions have been imposed at the ground level, thereby ignoring the initial base drift. Because of this assumption, the CSA method tends to largely overestimate the demands at the base as the soil becomes softer, as shown in Figs. 12 to 15. It is also not capable of estimating the demands of columns in underground storeys. However, regardless of the forces computed in the columns, they may not govern the design over the plastic hinge zone of shear walls or coupled walls. CSA A23.3-14 [6] indeed requires that columns and bearing walls have a curvature capacity greater than the curvature demand associated with the inelastic rotational demand in the SFRS over the plastic hinge zone.

7.3. Effect of cracked underground structure

Even if the aboveground part of the shear walls is usually designed with uncracked section properties of the underground structure, using cracked section properties may increase the displacements and thus the demands in the GLRS. Hence, analyses have been conducted with severely cracked section properties of the underground structure for all cases, as shown in Table 4. The interstorey drift and the flexural moment in corner column F6 and interior column C5 in the cantilever wall direction are shown in Figs. 16, 17 and 18. Only these results are presented, as they well represent the effects of a severely cracked underground structure.

When the underground structure is severely cracked, for the interstorey drift (Fig. 16), the flexibility of the foundation has stronger effects. Even for class C soil, there is a difference in the results between the SS, RO and FIX models. In comparison with the same results with an uncracked underground structure (Fig. 10), FIX models tend to more strongly overestimate the interstorey drift compared to NLTHA. This overestimation is especially large for class

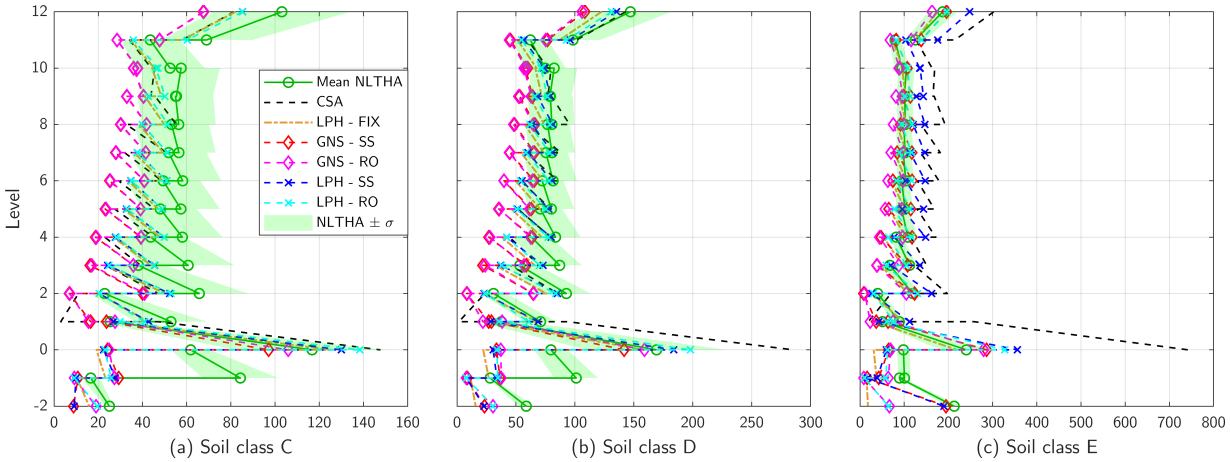

Figure 14: Flexural moment, in kNm, in column C5 for the cantilever wall direction with uncracked section properties of the underground structure. [Colour online].

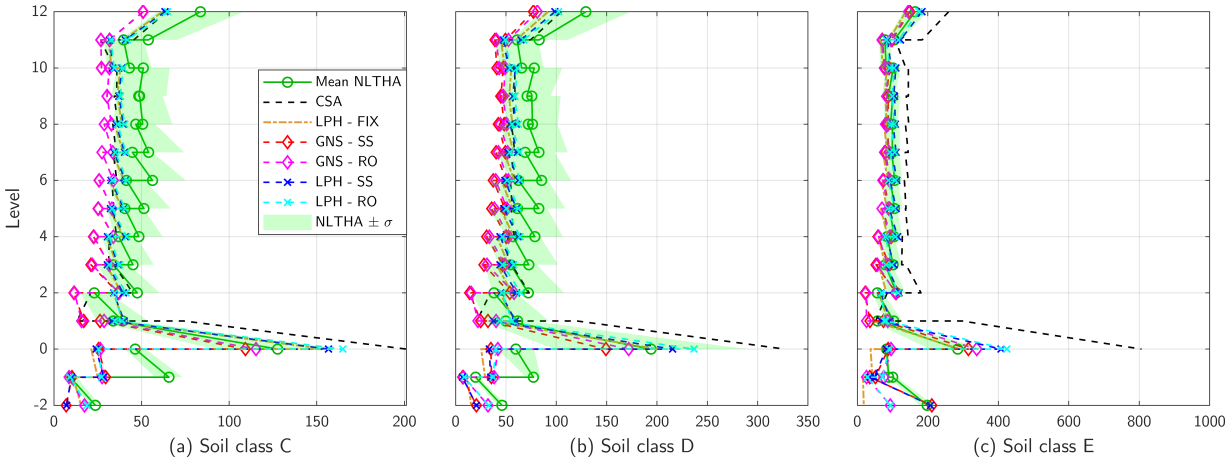

Figure 15: Flexural moment, in kNm, in column E3 for the coupled wall direction with uncracked section properties of the underground structure. [Colour online].

E soil (Fig. 16c), except for the LPH_FIX model, which ignores foundation movements. The peak at the first level for class E soil is explained later in this section.

In Fig. 16, it is clear that the interstorey drift computed with NLTHA shows more rotation at the base than with the uncracked underground structure (Fig. 10). This shows that the flexural moment at the ground level in the corner column computed with NLTHA (Figs. 17) increases by approximately 50% compared to the results with the uncracked underground structure (Fig. 12). This could be expected, as this column extends in the rigid foundation walls. However, for the interior column (Figs. 14 and 18) the opposite behaviour is observed. As the relative stiffness of the column to the slab increases when the underground structure is cracked, the forces developed in the column decrease at the ground level but tend to increase in the underground storeys.

For the upper levels, the flexural moments in columns F6 and C5 (Figs. 17 and 18) are well represented with all

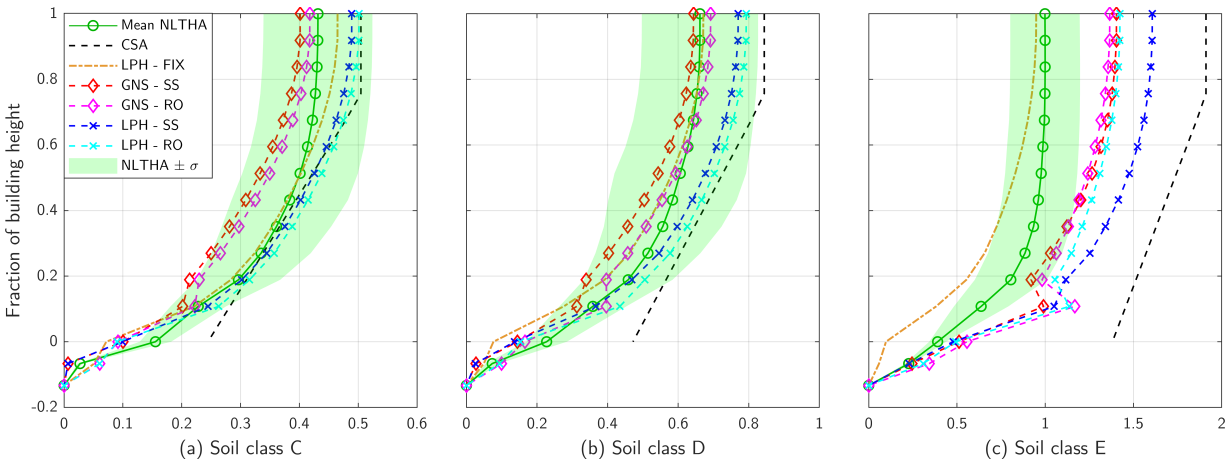

Figure 16: Lateral interstorey drift ratio, in percentage, for the cantilever wall direction with severely cracked section properties of the underground structure. [Colour online].

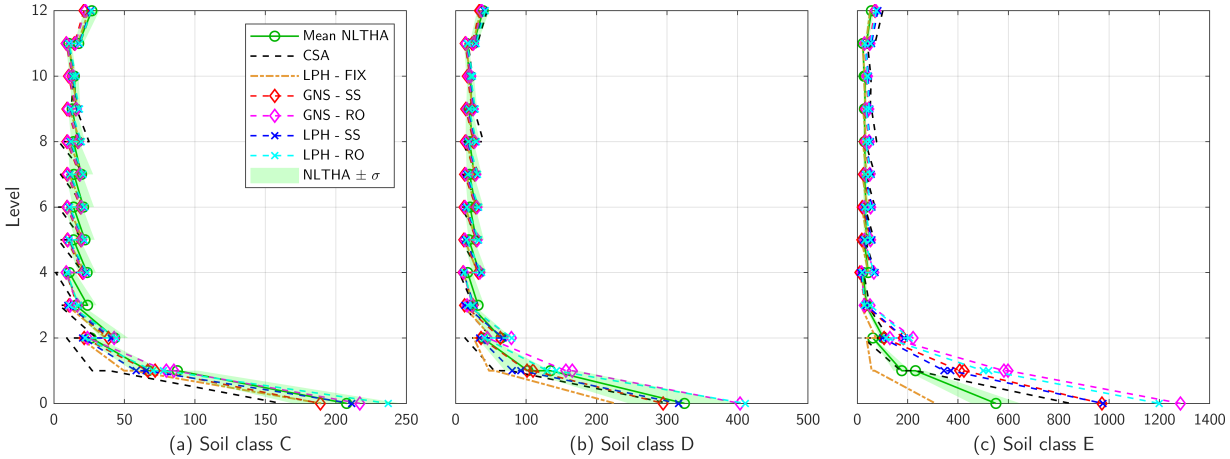

Figure 17: Flexural moment, in kNm, in column F6 for the cantilever wall direction with severely cracked section properties of the underground structure. [Colour online].

models compared to NLTHA. However, at the ground level, the behaviour shown by NLTHA is not well captured when the underground structure is severely cracked. The LPH_RO and GNS_RO models always overestimate the demands on the column, being worse as the soil becomes softer. LPH_SS, GNS_SS and CSA better model the demands but still overestimate them for class E soil. Only the LPH_FIX model, which ignores foundation movements, remains similar to NLTHA.

The large amplification shown by the SS and RO models when the underground structure is severely cracked (Figs. 17 and 18) can be explained through inspection of the modal results in the response spectrum analysis. The forces in the columns at the grade level are mainly controlled by the first vibration mode, which is shown conceptually in Fig. 19. This first vibration mode shows an important displacement of the core compared to the foundation walls at the ground level, and this effect becomes worse as the soil becomes softer. This means that the corner column has

Figure 18: Flexural moment, in kNm, in column C5 for the cantilever wall direction with severely cracked section properties of the underground structure. [Colour online].

almost no initial rotation at its base and that it suffers a large displacement between the first and ground level, as shown in Fig. 19. This also explains the peak at the first level in the interstorey drift curves, clearly visible in Fig. 16. For the interior column C5, the gap at the ground level for the SS and RO methods could partly be explained by the same reasoning. However, there is another cause of that gap. The stiffness of the columns of the ground level are reduced by an important factor according to the procedure proposed by Beauchamp et al. [10]; however, the stiffness of the ground level slab cannot be reduced by the same factor because its properties are used to define the stiffness of the underground level diaphragms. This implies that the ground-level slab restrains the columns more so than expected, leading to a higher moment demand at the base of the columns. In NLTHA, the GLRS is not reduced; therefore, a realistic relative stiffness of the slab-column nodes is conserved.

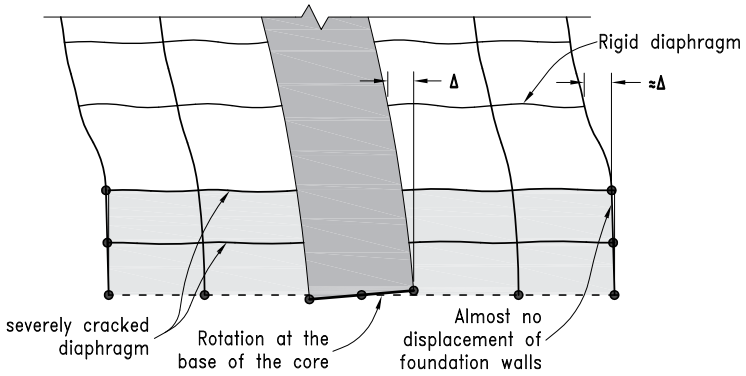

Figure 19: Relative displacement of the core to the foundation walls in the first vibration mode deformed shape.

8. Conclusions

This paper presents a complete and simple method for computing seismic demands in elements not part of the SFRS including foundation movements. Based on the method first proposed by Beauchamp et al. [10], this paper compares different models for considering foundation movements on linear soil media such as a simple rotational spring under each core (RO) or a complete set of springs and dashpots (SS). A fixed-base model including underground storeys (LPH_FIX) is also compared. These models are evaluated for a typical building by several NLTHAs in which SSI is modelled by a set of springs and dashpots, and ground motions are selected by the conditional spectrum method. NLTHAs are performed for soil classes ranging from stiff to soft (C, D and E according to NBCC 2015), and the effect of underground structure cracking is investigated by performing analyses on an uncracked and severely cracked underground structure. Additionally, all cases are used to assess the simplified method suggested in CSA A23.3-14. From the analysis results, the following conclusions can be drawn:

1. Using the linear plastic hinge approximation (LPH) is important in all proposed methods to obtain conservative results.
2. Modelling foundation movements is important for soft soils. Overall, the SS models give better results compared to NLTHA, but the RO models give a reasonable upper bound estimate considering the simplicity of its implementation. The FIX model may still be used, but it underestimates the demands. An amplification factor may be needed.
3. Using the cracked section properties of the underground structure leads to a larger flexural moment demand at the base of the columns that extends in foundation walls and in underground columns. On the other hand, uncracked section properties of the underground structure lead to a larger flexural moment demand at the ground level for columns that extend in the underground storeys.
4. Methods based on response spectrum analysis in which foundation movements are modelled and in which the severely cracked section properties of the underground structure are considered should be used with care. Important amplifications at the base of ground-level columns may appear because of the relative movement of the core inside the underground structure in the deformed shape of the first vibration mode.
5. The simplified method proposed in CSA A23.3-14 is quite cumbersome to implement. It produces satisfactory results for a stiff soil but largely overestimates the demands for a soft soil.

Based on these results, the most efficient method of computing demands in the GLRS is to use the method proposed by Beauchamp et al. [10] in a model that includes the underground storeys, in which the effects over the plastic hinge zone is reduced. Foundation movements should be explicitly considered for soil class D and softer. Then, at least a single rotational spring should be assigned under each core, or a complete set of springs and dashpots can be specified. If a fixed-base model is used, the forces calculated in the columns of the first storeys should be amplified. For the purpose of computing demands in the GLRS, underground structure cracking should be considered, as it leads to greater demands in certain components and is more realistic. When a building is analysed on a very soft soil, as in

class E in this paper, the behaviour of the GLRS is poorly captured by simpli ed linear methods. Hence, for class E soil, nonlinear analysis is required. However, many other analyses on other buildings, in which parameters such as the height, number of underground storeys and layout con guration are varied, would be needed to more fully assess the procedure proposed herein to consider foundation movements.

Acknowledgements

The authors would like to acknowledge the nancial support from the Natural Sciences and Engineering Research Council of Canada (NSERC) and the Fonds de recherche du Québec - Nature et technologies (FRQNT). Support from the Centre de recherche en génie parasismique et en dynamique des structures (CRGP) of the Université de Sherbrooke is also acknowledged.

References

[1] ASCE, ASCE/SEI 7-16 Minimum design loads for buildings and other structures, American Society of Civil Engineers : Structural Engineering Institute, 2016. URL https://doi.org/10.1061/9780784414248 .

[2] NRCC, National Building Code of Canada 2015, National Research Council Canada and Canadian Commission on Building and Fire Codes, Ottawa, ON, Canada, 2015.

[3] D. Mitchell, R. H. DeVall, M. Saatcioglu, R. Simpson, R. Tinawi, R. Tremblay, Damage to concrete structures due to the 1994 Northridge earthquake, Canadian Journal of Civil Engineering 22 (1995) 361–377. doi:10.1139/l95-047 .

[4] B. Boulanger, C.-P. Lamarche, J. Proulx, P. Paultre, Analysis of a damaged 12-storey frame-wall concrete building during the 2010 Haiti earthquake Part I: Dynamic behaviour assessment, Canadian Journal of Civil Engineering 40 (2013) 791–802. doi:10.1139/cjce-2012-0098 .

[5] K. J. Elwood, Performance of concrete buildings in the 22 February 2011 Christchurch earthquake and implications for Canadian codes, Canadian Journal of Civil Engineering 40 (2013) 759–776. doi:10.1139/cjce-2011-0564 .

[6] CSA, Design of concrete structures: CSA A23.3-14, Canadian Standards Association, Mississauga, ON, 2014.

[7] ACI committee 318, ACI 318-14: Building Code Requirements for Structural Concrete and Commentary, American Concrete Institute, Farmington Hills, MI, 2014.

[8] P. Adebar, P. Bazargani, J. Mutrie, D. Mitchell, Safety of gravity-load columns in shear wall buildings designed to Canadian standard CSA A23.3, Canadian Journal of Civil Engineering 37 (2010) 1451–1461. doi:10.1139/L10-075 .

[9] E. Dezhdar, Seismic response of cantilever shear wall buildings, Ph.D. thesis, University of British Columbia, Vancouver, 2012.

[10] J. Beauchamp, P. Paultre, P. Léger, A simple method for determining seismic demands on gravity load frames, Canadian Journal of Civil Engineering 44 (2017) 661–673. doi:10.1139/cjce-2016-0034 .

[11] J. P. Stewart, D. B. Chu, S. Lee, J. Tsai, P. Lin, B. Chu, R. E. Moss, R. B. Seed, S. Hsu, M. Yu, M. C. Wang, Liquefaction and non-liquefaction from 1999 Chi-Chi, Taiwan, earthquake, in: Proceedings of the Sixth U.S. Conference and Workshop on Lifeline Earthquake Engineering, August 10, 2003 - August 13, 2003, Technical Council on Lifeline Earthquake Engineering Monograph, American Society of Civil Engineers, 2003, pp. 1021–1030. doi:10.1061/40687(2003)103 .

[12] P. Paultre, G. Lefebvre, J.-P. Devic, G. Cote, Statistical analysis of damages to buildings in the 1988 Saguenay earthquake, Canadian Journal of Civil Engineering 20 (1993) 988–998. doi:10.1139/l93-130 .

[13] S. Marzban, M. Banazadeh, A. Azarbakht, Seismic performance of reinforced concrete shear wall frames considering soil-foundation-structure interaction, Structural Design of Tall and Special Buildings 23 (2014) 302–318. doi:10.1002/tal.1048 .

[14] CAC, Concrete Design Handbook, 4th ed., Cement Association of Canada, Ottawa, 2016.

[15] P. Adebar, Nonlinear rotation of capacity-protected foundations: the 2015 Canadian building code, Earthquake Spectra 31 (2015) 1885–1907. doi:10.1193/012814EQS022M

[16] NEHRP Consultants Joint Venture, Soil-Structure Interaction for Buildings Structures, Technical Report NIST GCR 12-917-21, National Istitute of Standards and Technology, 2012. URL: https://www.nehrp.gov/pdf/nistgcr12-917-21.pdf .

[17] B. Fatahi, H. R. Tabatabaiefar, B. Samali, Soil-structure interaction vs sta e for seismic design of tall buildings on soft soil, Geomechanics and Engineering 6 (2014) 293–320. URL: http://dx.doi.org/10.12989/gae.2014.6.3.293 .

[18] S. Ghosh, E. L. Wilson, Dynamic stress analysis of axisymmetric structures under arbitrary loading, Technical Report EERC 69-10, University of California, Berkeley, California, 1969.

[19] P. Paultre, M. Lavoie, E ects of soil-structure interaction on the seismic performance of a concrete frame-wall structure, in: Proceedings of the Sixth Canadian Conference on Earthquake Engineering, 12 - 14 June 1991, Toronto, Univ. of Toronto Press, Toronto, 1991, pp. 405–412.

[20] J. Lysmer, R. L. Kuhlemeyer, Finite dynamic model for in nite media, Journal of the Engineering Mechanics Division 95 (1969) 859–878.

[21] E. L. Wilson, Three-dimensional static and dynamic analysis of structures: a physical approach with emphasis on earthquake engineering, CSI, Berkeley, Calif., 2002.

[22] P. Léger, M. Boughoufalah, Earthquake input mechanisms for time-domain analysis of dam-foundation systems, Engineering Structures 11 (1989) 37–46. doi:10.1016/0141-0296(89)90031-X .

[23] G. A. Ordonez, SHAKE2000 A Computer Program for the 1-D Analysis of Geotechnical Earthquake Engineering Problems, 2011. URL: http://www.geomotions.com/index.php .

[24] Y. M. Hashash, M. I. Musgrove, J. A. Harmon, D. Groholski, C. A. Phillips, D. Park, DEEPSOIL v6.1, User Manual, Technical Report, University of Illinois, Urbana, IL, 2015.

[25] G. S. Sooch, A. Bagchi, A New iterative procedure for deconvolution of seismic ground motion in dam-reservoir-foundation systems, Journal of Applied Mathematics 2014 (2014) 1–10. doi:10.1155/2014/287605 .

[26] R. B. Reimer, Deconvolution of seismic response for linear systems, Technical Report EERC 73-10, University of California, Berkeley, California, 1973.

[27] A. Pais, E. Kausel, Approximate formulas for dynamic stiffnesses of rigid foundations, International Journal of Soil Dynamics and Earthquake Engineering 7 (1988) 213–227. doi:10.1016/S0267-7261(88)80005-8 .

[28] G. Gazetas, Formulas and charts for impedances of surface and embedded foundations, Journal of Geotechnical Engineering 117 (1991) 1363–1381. doi:10.1061/(ASCE)0733-9410(1991)117:9(1363) .

[29] G. Mylonakis, S. Nikolaou, G. Gazetas, Footings under seismic loading: Analysis and design issues with emphasis on bridge foundations, Soil Dynamics and Earthquake Engineering 26 (2006) 824–853. doi:10.1016/j.soildyn.2005.12.005 .

[30] Computers and Structures inc., SAP2000 Ultimate v18.2.0, 2016. URL: https://www.csiamerica.com/products/sap2000 .

[31] A. T. C. (ATC), Modeling and acceptance criteria for seismic design and analysis of tall buildings, Technical Report ATC-72-1, Paci c Earthquake engineering Research Center (PEER), Redwood City, CA., 2010.

[32] B. Fatahi, H. R. Tabatabaiefar, E ects of soil plasticity on seismic performance of mid-rise building frames resting on soft soils, Advances in Structural Engineering 17 (2014) 1387–1402. URL: http://dx.doi.org/10.1260/1369-4332.17.10.1387 .

[33] S. H. R. Tabatabaiefar, B. Fatahi, B. Samali, Seismic behavior of building frames considering dynamic soil-structure interaction, ASCE International Journal of Geomechanics 13 (2012) 409–420. URL: http://dx.doi.org/10.1061/(ASCE)GM.1943-5622.0000231 .

[34] Itasca Consulting Group, Minneapolis, FLAC2D: Fast Lagrangian analysis of continua, version 6.0., 2008.

[35] H. R. Tabatabaiefar, B. Fatahi, K. Ghabraie, W. Zhou, Evaluation of numerical procedures to determine seismic response of structures under in uence of soil-structure interaction, Structural Engineering and Mechanics 56 (2015) 27–47. doi:10.12989/sem.2015.56.1.027.

[36] H. R. Tabatabaiefar, T. Clifton, Signi cance of considering soil-structure interaction e ects on seismic design of unbraced building frames resting on soft soils, Australian Geomechanics Journal 51 (2016) 55–56. URL: http://hdl.handle.net/10453/53007 .

[37] S. H. R. Tabatabaiefar, A. A. Massumi, A simpli ed method to determine seismic responses of reinforced concrete moment resisting

building frames under in uence of soil-structure interaction, Soil Dynamics and Earthquake Engineering 30 (2010) 1259–1267. URL: doi.org/10.1016/j.soildyn.2010.05.008 .

[38] LATBSDC, An alternative procedure for seismic analysis and design of tall buildings located in the Los Angeles region - a consensus document, Technical Report, Los Angeles Tall Buildings Structural Design Council, 2017 with 2018 Supplements.

[39] Seismosoft, SeismoStruct 2016 - A computer program for static and dynamic nonlinear analysis of framed structures, 2016. Available from http://www.seismosoft.com.

[40] D. Naish, A. Fry, R. Klemencic, J. Wallace, Reinforced concrete coupling beams-part II: modeling, ACI Structural Journal 110 (2013) 1067–75. doi:10.14359/51686161 .

[41] N. Son Vu, B. Li, K. Beyer, Eective sti ness of reinforced concrete coupling beams, Engineering Structures 76 (2014) 371–382. doi: 1016/j.engstruct.2014.07.014 .

[42] J. Mander, M. Priestley, R. Park, Theoretical stress-strain model for con ned concrete, Journal of Structural Engineering 114 (1988) 1804–1826. doi:10.1061/(ASCE)0733-9445(1988)114:8(1804) .

[43] M. Menegetto, P. E. Pinto, Method of analysis for cyclically loaded RC plane frames including changes in geometry and non-elastic behavior of elements under combined normal force and bending, in: Symposium on resistance and ultimate deformbility of structures acted on by well de ned repeated loads, International Association for Bridge and Structural Engineering, Zurich, Switzerland, 1973, pp. 15–22.

[44] F. C. Filippou, E. P. Popov, V. V. Bertero, Eects of bond deterioration on hysteretic behavior of reinforced concrete joints, Technical Report EERC 83-19, University of California, Berkeley, California, 1983.

[45] Seismosoft, SeismoStruct - User Manual, Technical Report, Seismosoft, Italy, 2016.

[46] Computers and Structures inc., ETABS Ultimate 2016 v16.0.2, 2016. URL: https://www.csiamerica.com/products/etabs .

[47] J. W. Baker, Conditional mean spectrum: Tool for ground-motion selection, Journal of Structural Engineering 137 (2011) 322–331. doi: 1061/(ASCE)ST.1943-541X.0000215.

[48] J. W. Baker, C. Lee, An improved algorithm for selecting ground motions to match a conditional spectrum, Journal of Earthquake Engineering (2017) 1–16. doi:10.1080/13632469.2016.1264334 .

[49] MathWorks, MATLAB R2016a, 2016. URL: https://www.mathworks.com/products/new_products/release2016a.html .

[50] Global Earthquake Model Foundation, OpenQuake Engine 2.5.0, 2017. URL: https://old.globalquakemodel.org/openquake/start/download/ .

[51] G. Atkinson, J. Adams, Ground motion prediction equations for application to the 2015 Canadian national seismic hazard maps, Canadian Journal of Civil Engineering 40 (2013) 988–98. doi:10.1139/cjce-2012-0544 .

[52] C. Bernier, R. Monteiro, P. Paultre, Using the conditional spectrum method for improved fragility assessment of concrete gravity dams in Eastern Canada, Earthquake Spectra 32 (2016) 1449–1468. doi:10.1193/072015EQS116M

[53] Paci c Earthquake Engineering Research Center (PEER), PEER Ground Motion Database, 2014. URL: http://ngawest2.berkeley.edu/ .

[54] S. Halchuk, T. I. Allen, J. Adams, G. C. Rogers, Fifth generation seismic hazard model input les as proposed to produce values for the 2015 national building code of Canada, Technical Report 7576, Geological Survey of Canada, 2014. doi:10.4095/293907 .

[55] D. M. Boore, G. M. Atkinson, Ground-motion prediction equations for the average horizontal component of PGA, PGV, and 5%-damped PSA at spectral periods between 0.01 s and 10.0 s, Earthquake Spectra 24 (2008) 99–138. doi:10.1193/1.2830434 .

[56] Y. Choi, J. P. Stewart, Nonlinear site ampli cation as function of 30 m shear wave velocity, Earthquake Spectra 21 (2005) 1–30. doi: 1193/1.1856535 .